A&A 410, 415–424 (2003)
DOI: 10.1051/0004-6361:20031197

Astronomy & Astrophysics

Linear damping and energy dissipation of shear Alfvén waves in the interstellar medium

M. Lazar[1], F. Spanier[2], and R. Schlickeiser[2]

[1] Alexandru Ioan Cuza University, Faculty of Physics, Bd. Carol I Nr. 11, 6600 Iasi, Romania
[2] Institut für Theoretische Physik, Lehrstuhl IV: Weltraum- und Astrophysik, Ruhr-Universität Bochum, 44780 Bochum, Germany
e-mail: r.schlickeiser@tp4.rub.de, fspanier@tp4.rub.de

Received 6 January 2003 / Accepted 31 July 2003

Abstract. The heating of the diffuse interstellar medium by the dissipation of interstellar shear Alfvén waves is an important process for the temperature balance of this gas phase. Following our earlier analysis for fast magnetosonic waves we calculate here the heating rate from the damping of interstellar shear Alfvén waves, because interstellar plasma turbulence most probably is a mixture of fast magnetosonic waves and shear Alfvén waves. Relating the Alfvénic magnetic field fluctuation power spectrum to the observed interstellar electron density fluctuation power spectrum we derive the heating rate allowing for a scale independent anisotropy of the power spectrum. Because the diffuse intercloud medium is a partially ionised medium, the shear Alfvén waves undergo different types of dissipation. Besides collisionless Landau damping we considered various damping mechanisms from collision-effects such as Joule dissipation, electron and ion viscosity and ion-neutral friction. For all individual damping processes we derive the respective damping rates as a function of wavenumber and propagation angles of the Alfvén waves. These damping rates then serve as input in the calculation of the associated heating rates of the interstellar medium which results from the integral over the product of the damping rate times the magnetic field fluctuation power spectrum allowing for a scale independent anisotropy of the power spectrum. We demonstrate that for isotropic turbulence and typical diffuse intercloud medium parameters ion-neutral friction provides the dominant contribution to the heating rate of about 10^{-29} erg cm^{-3} s^{-1}, which is about four orders of magnitude smaller than the cooling rate of the diffuse intercloud medium. Heating by collisionless Landau damping is 13 orders of magnitude smaller than dissipation by ion-neutral friction, heating by Joule and viscosity dissipation is 10 orders of magnitude smaller. Apart from factors of order unity these heating rates also hold for predominantly parallel turbulence ($\Lambda \gg 1$). In case of predominantly perpendicular turbulence ($\Lambda \ll 1$) the heating rates from collisionless Landau damping and Joule and viscosity dissipation decrease $\propto \Lambda^{1/2}$, whereas the heating rate from ion-neutral friction increases $\propto \Lambda^{-s/2}$ as long as $\Lambda \geq 10^{-6}$. However, compared to the heating rate by collisionless Landau damping of fast magnetosonic waves the heating rate of Alfvén waves is negligibly small. Hence, for the temperature balance of the warm intercloud medium heating from shear Alfvén waves is negligible compared to the heating by collisionless damping of fast magnetosonic waves.

Key words. magnetohydrodynamics (MHD) – plasmas – turbulence – waves – ISM: general – ISM: magnetic fields

1. Introduction

The interstellar medium consists of at least three distinct phases in approximate pressure equilibrium: cold clouds, warm intercloud medium, and hot coronal gas generated by supernova explosions. 21 cm radio studies indicate that the warm medium has a temperature between 6000 and 10^4 K and a mean HI-density of about 0.8 cm^{-3}, but is very stuctured in colder clouds and a warm intercloud medium of density 0.1–0.2 cm^{-3}. Under such conditions atomic and metallic radiative transitions efficiently cool the gas, so that an efficient heating mechanism is required in order to maintain the gas temperature.

Various heating mechanisms of the interstellar medium have been suggested, including background ultraviolet and X-ray heating (e.g. Cheng & Bruhweiler 1990), cosmic ray heating (e.g. Lerche & Schlickeiser 1982), and photoelectric emission from grains. Recently, Lerche & Schlickeiser (2001 – hereafter referred to as Paper I) have investigated the heating of the warm gas by the collisionless damping of interstellar fast magnetosonic waves. They demonstrated that the fast magnetosonic wave energy loss rates agree well with the cooling rates for the fluctiferous (H II) and the diffuse interstellar medium when the anisotropy in the magnetosonic wave power spectrum is properly accounted for. Their calculations apply to the stationary interstellar medium with large spatial scales and without strong spatial inhomogenities, i.e. far away from phase boundaries and shock waves, so that to a first approximation the

Send offprint requests to: R. Schlickeiser,
e-mail: rsch@tp4.ruhr-uni-bochum.de

equilibrium temperature is determined by the simple balance of heating and cooling rates

$$\epsilon(\rho, T) = \lambda(\rho, T). \quad (1)$$

It is the purpose of the present investigation to calculate (analogously to the analysis in Paper I for fast magnetosonic waves) the heating of the warm gas by the collisionless damping of interstellar shear Alfvén waves, because interstellar plasma turbulence most probably is a mixture of fast magnetosonic waves and shear Alfvén waves. In order to avoid unnecessary repitions we will use the same notation and will frequently refer to equations in Paper I.

As in Paper I we adopt a power spectrum of electron density fluctuation in the form

$$P_{\rm nn}(\boldsymbol{k}) = C_{\rm N}^2 \left[k_\parallel^2 + \Lambda k_\perp^2\right]^{-(2+s)/2}. \quad (2)$$

Here $k_\parallel$ ($k_\perp$) is the wavenumber parallel (perpendicular) to the ambient magnetic field; s is the spectral index; Λ is the anisotropy parameter. Isotropy occurs if $\Lambda = 1$, whereas if the wave turbulence is more along the lines of thin "platelets" paralleling the ambient field, as suggested by Goldreich & Sridhar (1995), then $\Lambda \gg 1$. The constant $C_{\rm A}^2$ is such that

$$\int {\rm d}^3k\, P_{\rm nn}(\boldsymbol{k}) = (\delta n_{\rm e})^2 \quad (3)$$

where $\delta n_{\rm e}$ denotes the total fluctuating electron density. The form of the wave spectrum given by Eq. (2) is taken to operate only between some small wavenumber, $k = k_{\rm min}$, and a large wavenumber, $k = k_{\rm max}$, with $k = |\boldsymbol{k}| = [k_\parallel^2 + k_\perp^2]^{1/2}$. Spangler (1991) suggests that these wavenumbers are related to outer and inner scale lengths, $l_{\rm min}$ and $l_{\rm max}$, respectively, with $l_{\rm min} = 2\pi/k_{\rm max}$, $l_{\rm max} = 2\pi/k_{\rm min}$. The physical bounds of $l_{\rm min}$ and $l_{\rm max}$ are not precisely known, but probably related to the Whistler wave resonance limit of the interstellar electrons and the physical size of the warm intercloud medium i.e. the mean cloud distance, respectively. The inner scale is estimated by Spangler (1991) to be of the general order of $l_{\rm min} = 10^7 l_7$ cm, ($l_7 = 1$), with the outer scale of order $l_{\rm max} = 10^{17} L_{17}$ cm with $L_{17} = 1$ in hot, ionized regions, and $L_{17} = 30$ in the diffuse phase of the interstellar medium. In our study here we assume that the power spectrum (2) holds in the stationary and homogenous warm intercloud medium.

The power spectrum itself results from the balance of all wave damping and driving processes, including in particular the non-linear energy tranfer from large turbulence scales to small scales. Our calculation presented here is limited in the sense that we assume a given and fixed power spectrum to determine the heating rate of the interstellar medium, but we do not self-consistently investigate the processes leading to the formation of the power spectrum. In particular, we do not consider non-linear damping of waves associated with turbulent interactions or with non-linear plasma wave amplitude effects (see e.g. Lerche & Schlickeiser 2002). This work assumes that these non-linear effects are less important than the linear damping rates. Therefore, our calculated heating rate from linear damping processes only provides a lower boundary of heating associated with the spectrum of Alfvén waves. The upper boundary is achieved when the non-linear energy transfer along the cascade and the associated damping occur over a single wave period. The latter is a corner stone of the Goldreich-Sridhar model of turbulence.

Nevertheless, we regard our calculation of the heating rate of the warm phase of the interstellar medium by linear Alfvén wave damping processes as a valuable addition to the existing research in this field mainly for two reasons:

First, our work may be relevant to the actual heating of the interstellar medium as the recent work on magnetohydrodynamic turbulence by Cho et al. (2002) has demonstrated that the turbulence may decay non-linearly much slower than its maximal rate above, provided the cascade is imbalanced. In this situation the linear damping might get important for media heating.

Secondly, our calculations clarify the respective roles of collisionless wave damping processes (i.e. Landau damping) and damping associated with collision-effects associated with Joule dissipation, electron and ion viscosity and ion-neutral friction, respectively, in the partially ionised warm phase of the interstellar medium.

2. Relation of interstellar electron density and magnetic field fluctuations

Within a plasma wave viewpoint this interstellar turbulence is a mixture of fast magnetosonic waves and shear Alfvén waves because the plasma beta $\beta = 0.22$ of the diffuse interstellar intercloud phase is much smaller unity. In order to calculate the wave energy dissipation rate the power spectrum of the associated magnetic field fluctuations is the important input quantity (see Eq. (9) below). However, accessible from the observations is only the power spectrum (2) of interstellar electron density fluctuations. Therefore, we first have to discuss the relation of interstellar electron density and magnetic field fluctuations for these two types of plasma waves.

According to classical MHD theory (Sturrock 1961, Ch. 14.1) shear Alfvén waves are incompressible ($\delta n_{\rm e} = 0$) whereas fast magnetosonic waves for low-beta plasma exhibit a direct correspondence $\delta n_{\rm e}/n_{\rm e} \simeq \delta B_{\rm z}/B_0$ between electron density fluctuations and the fluctuations in the parallel fluctuating magnetic field component. However, because the plasma parameter $g = \nu_{\rm ee}/\omega_{\rm p,e} \simeq 10^{-10}$ of the diffuse intercloud gas is much smaller than unity, a full kinetic description rather than the MHD description of the plasma turbulence at turbulence spatial scales $l < l_{\rm MHD} \simeq 0.003$ pc is necessary. Recently, using linear kinetic plasma theory Schlickeiser & Lerche (2002) calculated the relation between the magnetic field fluctuation and electron density fluctuation power spectra for shear Alfvén waves and fast magnetosonic waves which are the two magnetohydrodynamic plasma wave modes at frequencies well below the non-relativistic proton frequency. If the respective waves propagate at an angle θ with respect to the uniform background magnetic field $\boldsymbol{B}_0 = B_0 \boldsymbol{e}_{\rm z}$ they obtained for shear Alfvén

$$\frac{P_{\rm yy}^{\rm A}(\boldsymbol{k})}{B_0^2} = \frac{\Omega_{\rm p}^2 \sin^2\theta}{9 V_{\rm A}^2 k^2} \frac{P_{\rm nn}^{\rm A}(\boldsymbol{k})}{n_{\rm e}^2} \quad (4)$$

whereas for fast magnetosonic waves at propagation angles $\theta \leq$ 86 degrees

$$\frac{P_{zz}^{M}(\boldsymbol{k})}{B_0^2} = \tan^2\theta \frac{P_{xx}^{M}(\boldsymbol{k})}{B_0^2} = \frac{1}{9\left[1+\beta\sin^2\theta\right]^2}\frac{P_{nn}^{M}(\boldsymbol{k})}{n_e^2} \simeq \frac{P_{nn}^{M}(\boldsymbol{k})}{9n_e^2} \quad (5)$$

where the latter approximation holds for small plasma beta $\beta \ll 1$. As an aside we note that the analytic result (4) of Schlickeiser & Lerche (2002) for low-beta plasmas corresponds to a similar result from the numerical study of Gary (1995) of an increasing compressibility of obliquely propagating shear Alfvén waves with increasing wavenumber in a high-beta plasma.

Using the relations (4) and (5) we immediately deduce the corresponding magnetic field power spectra of shear Alfvén waves and fast magnetosonic waves as

$$P_{yy}^{A}(\boldsymbol{k}) = C_A^2 \frac{k_\perp^2 k_c^2}{k^4\left[k_\parallel^2+\Lambda k_\perp^2\right]^{(2+s)/2}}, \quad (6)$$

where the characteristic wavenumber scale $k_c = \Omega_p/V_A = \omega_{p,i}/c$ denotes the inverse interstellar ion skin length, and

$$P_{zz}^{M}(\boldsymbol{k}) = C_M^2\left[k_\parallel^2+\Lambda k_\perp^2\right]^{-(2+s)/2} \quad (7)$$

with

$$C_A^2 + C_M^2 = \left(\frac{B_0}{3n_e}\right)^2 C_N^2. \quad (8)$$

Obviously, the constants C_A and C_M determine the values of the total magnetic field fluctuation energy density in shear Alfvén waves $(\delta B)_A^2$ and fast magnetosonic waves $(\delta B)_M^2$. For the diffuse intercloud medium Minter & Spangler (1997) have given the value $\delta B = \sqrt{(\delta B)^2} = 0.9\ \mu$G for the total fluctuating magnetic field strength; the respective contributions of shear Alfvén waves and fast magnetosonic waves are unknown. We note that for the given electron density fluctuation spectrum (2) as a function of wavenumber k the magnetic field fluctuation power spectrum of oblique shear Alfvén waves is steeper than the magnetic field fluctuation power spectrum of fast magnetosonic waves. In case of isotropic ($\Lambda = 1$) turbulence the Alfvénic magnetic field power spectrum scales $\propto k^{-s-4}$ with $s \simeq 5/3$ whereas the magnetic field power spectrum of fast magnetosonic waves scales as $\propto k^{-s-2}$.

In the following we will use the power spectrum (6) as input quantity to calculate the Alfvén wave energy dissipation rate in the interstellar medium.

3. Alfvén wave damping rates

For waves damping at a rate $\gamma_0(\boldsymbol{k})$, the energy loss rate ϵ_0 is conventionally written in the form (Spangler 1991)

$$\epsilon_0 = \frac{1}{4\pi}\int \mathrm{d}^3k\, P_{yy}^{A}(\boldsymbol{k}) 2\gamma_0(\boldsymbol{k}). \quad (9)$$

The warm phase of the interstellar medium is a partially ionised plasma. The shear Alfvén waves undergo different types of dissipation in this low-temperature plasma: besides collisionless Landau damping (γ_A) there is damping connected with the collision-effects associated with Joule dissipation (γ_J), electron and ion viscosity (γ_V) (Braginskii 1965; Hollweg 1985) and ion-neutral friction (γ_N) (Kulsrud & Pearce 1969). The total damping rate for the shear Alfvén waves then is

$$\gamma_0 = \gamma_A + \gamma_J + \gamma_V + \gamma_N. \quad (10)$$

We discuss each contribution in turn.

3.1. Collisionless Landau damping

For an obliquely propagating shear Alfvén wave the damping rate is given by Ginzburg (1961, p. 218, Eq. (14.56)) as

$$\gamma = \left(\frac{\pi}{8}\right)^{1/2}\frac{\omega^3}{\Omega_p^2}\frac{v_e}{V_A}\frac{\tan^2\theta}{\sin^2\theta+3\left(\omega^2/\Omega_p^2\right)\cos^2\theta} \times\left[v_i^2/v_e^2+\left(\sin^2\theta+4\cos^2\theta\right)\exp\left[-V_A^2/\left(2v_i^2\cos^2\theta\right)\right]\right], \quad (11)$$

where $\sin\theta = |k_\perp|/k$, V_A is the Alfvén speed, v_i (v_e) is the ion (electron) thermal speed and $\Omega_p = eB/m_i c$ is the ion gyrofrequency. Conditions are also attached to the domain of validity of Eq. (11). These conditions, as spelled out by Ginzburg (1961), are:
(1) both ions and electrons are taken to be at the same temperature and both are described by isotropic Maxwellian distributions, $v_e = \sqrt{k_B T/m_e}$, $v_i = \sqrt{k_B T/m_i} = v_e(m_e/m_i)^{1/2}$;
(2) one must have $V_A \gg v_i$ and $v_e \gg v_i$;
(3) Eq. (11) is valid only in the angular range described through (Ginzburg 1961, p. 218, Eq. (14.54))

$$v_e|\cos\theta| \gg V_A|\cos\theta| \gg v_i|\cos\theta| \quad (12)$$

which correspond to

$$v_i \ll V_A \ll v_e. \quad (13)$$

The exponential factor $\exp[-V_A^2/(2v_i^2\cos^2\theta)]$ is exceedingly small for all values of θ, so, to a very accurate approximation, we obtain:

$$\gamma_A \simeq \left(\frac{\pi}{8}\right)^{1/2}\frac{v_i^2 k^3}{v_e k_c^2}\frac{\cos\theta\sin^2\theta}{\sin^2\theta+3\left(k^2/k_c^2\right)\cos^4\theta}, \quad (14)$$

where we have used the dispersion relation for the shear Alfvén waves, $\omega = kV_A\cos\theta$, and a critical wave number

$$k_c = \Omega_p/V_A = \omega_{p,i}/c = 4.4\times10^{-8}\sqrt{n_e}\,\mathrm{cm}^{-1} \quad (15)$$

has been defined.

In terms of the dimensionless wave number

$$\kappa \equiv k/k_c \quad (16)$$

the damping rate (14) reads

$$\gamma_A(k) \simeq \left(\frac{\pi}{8}\right)^{1/2}\frac{m_e}{m_p}v_e k_c \kappa^3\frac{\cos\theta\sin^2\theta}{\sin^2\theta+3\kappa^2\cos^4\theta}. \quad (17)$$

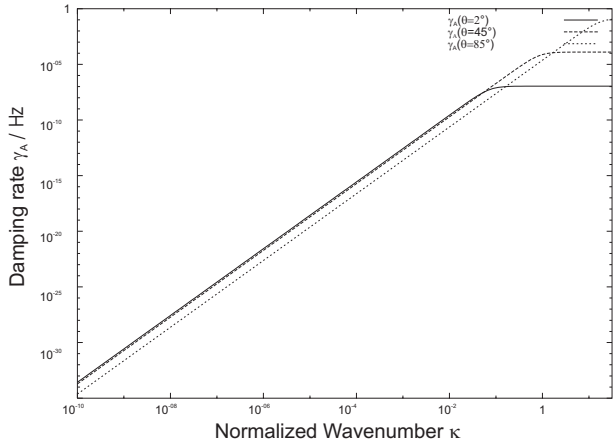

Fig. 1. Damping rate γ_A for collisionless Landau damping as a function of normalised wave number at three propagation angles.

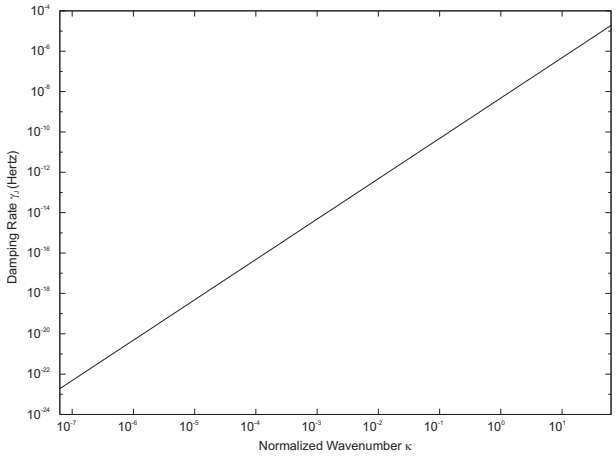

Fig. 2. Damping rate γ_{V+J} for Joule and viscous damping as a function of normalised wavenumber for wave propagation angle $\theta = 2°$.

We now use typical parameters for the intercloud medium: $n_e = 0.2\, n_{0.2}$ cm^{-3}, $T_e = 10^4\, T_4$ K and $B_0 = 4\, b_4\, \mu$G to obtain numerically $k_c = 2 \times 10^{-8}\, n_{0.2}^{1/2}$ cm^{-1} and

$$\gamma_A(\kappa) = 2.7 \times 10^{-4}\, T_4\, n_{0.2}^{1/2}\, \kappa^3 \frac{\cos\theta \sin^2\theta}{\sin^2\theta + 3\kappa^2 \cos^4\theta} \text{ Hz}. \quad (18)$$

The damping rate γ_A is plotted in Fig. 1 for the three angles 2°, 45° and 86°.

3.2. Joule dissipation

In terms of the electrical conductivities

$$\sigma_\perp = \frac{e^2 n_e}{m_e \nu_e} = \frac{\omega_{pe}^2}{4\pi\nu_e}, \quad \sigma_\parallel = 1.96\sigma_\perp \quad (19)$$

where $\omega_{p,e} = 5.64\sqrt{n_e}$ Hz is the electron plasma frequency and

$$\nu_e = 2.86 \times 10^{-5} n_e (L/10)(k_B T_e(\text{eV}))^{-3/2} \quad (20)$$

is the electron collision rate with the Coulomb logarithm,

$$L = 23.4 - 1.15 \lg n + 3.45 \lg k_B T_e(\text{eV}) \quad (21)$$

for $k_B T_e < 50$ eV, the Joule damping rate of Alfvén waves is (Braginskii 1965)

$$\gamma_J(k) = \frac{c^2 k^2}{8\pi}\left(\frac{\sin^2\theta}{\sigma_\parallel} + \frac{\cos^2\theta}{\sigma_\perp}\right) = \frac{\nu_e c^2 k^2}{2\omega_{p,e}^2}\left[\cos^2\theta + 0.51\sin^2\theta\right]. \quad (22)$$

In terms of the dimensionless wavenumber (16) and typical intercloud plasma parameters we obtain

$$\gamma_J(\kappa) = 4.8 \times 10^{-9}\, n_{0.2}\, T_4^{-3/2}\, \kappa^2 \left[\cos^2\theta + 0.51\sin^2\theta\right] \text{ Hz}. \quad (23)$$

3.3. Viscosity dissipation

The viscosity damping rate involves two of the five coefficients of the viscous stress tensor. Summing over the contributions from electron and ion viscosity we obtain from Braginskii (1965)

$$\gamma_V(k) = \frac{k^2}{2 m_p n_e}\left[(\eta_1(\text{p}) + \eta_1(\text{e}))\sin^2\theta + (\eta_2(\text{p}) + \eta_2(\text{e}))\cos^2\theta\right] = 0.15 \frac{k_B T_p}{m_p c^2} \frac{k^2 c^2 \tau_i}{(\Omega_{p,0}\tau_i)^2} \times \left[\sin^2\theta + 4\cos^2\theta\right]\left[1 + 0.17\left(\frac{m_e}{m_p}\right)^{3/2}\left(\frac{T_p}{T_e}\right)^{1/2}\right] \quad (24)$$

where

$$\tau_i = \nu_i^{-1} = \frac{2.12 \times 10^6}{(L/10)} \frac{\left(k_B T_p(\text{eV})\right)^{3/2}}{n_e} \quad (25)$$

and

$$\Omega_{p,0}\tau_i = \frac{4.07 \times 10^{10}}{(L/10)} \frac{B(\text{Gauss})(k_B T_p(\text{eV}))^{3/2}}{n_e} \quad (26)$$

denotes the ratio of proton gyrofrequency to collision rate.

For an equal temperature plasma, Eq. (24) reduces to

$$\gamma_V(k) \simeq 0.15 \frac{k_B T_p}{m_p c^2} \frac{k^2 c^2 \tau_i}{(\Omega_{p,0}\tau_i)^2}\left[\sin^2\theta + 4\cos^2\theta\right]. \quad (27)$$

In terms of the dimensionless wavenumber (16) and typical intercloud plasma parameters we obtain

$$\gamma_V(\kappa) = 10^{-7} n_{0.2}^2\, T_4^{-3/2}\, b_4^{-4}\, \kappa^2 \left[\sin^2\theta + 4\cos^2\theta\right] \quad (28)$$

which has the same wavenumber dependence as the Joule damping rate (23), and therefore for all values of κ is by a factor 40 larger than the Joule damping rate. In the following we therefore neglect the Joule damping rate with respect to the viscous damping rate, i.e. for the sum of both

$$\gamma_{V+J}(\kappa) \simeq \gamma_V(\kappa) = 10^{-7} n_{0.2}^2\, T_4^{-3/2} b_4^{-4}\, \kappa^2 \left[\sin^2\theta + 4\cos^2\theta\right]. \quad (29)$$

The variation with normalised wavenumber of the combined damping rate $\gamma_{V+J}(\kappa)$ for a propagation angle of 2° is shown in Fig. 2.

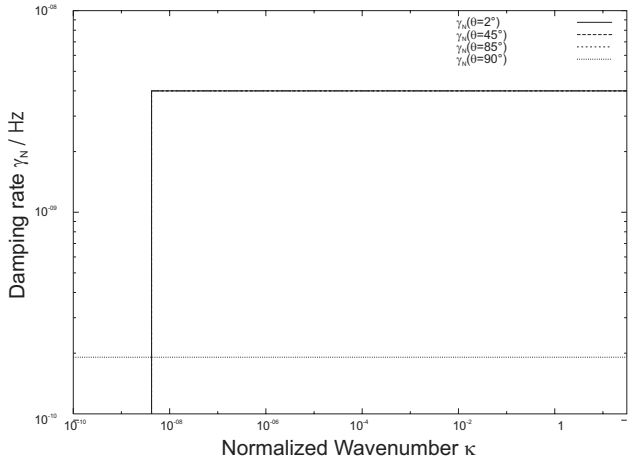

Fig. 3. Damping rate γ_N for ion neutral Damping.

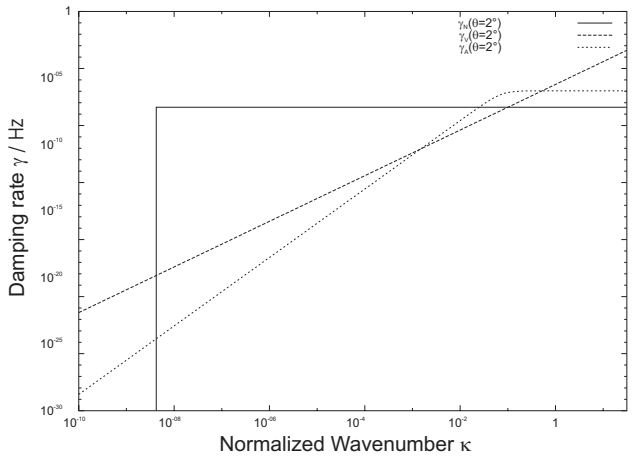

Fig. 4. Comparison of the damping rates at $\theta = 2°$.

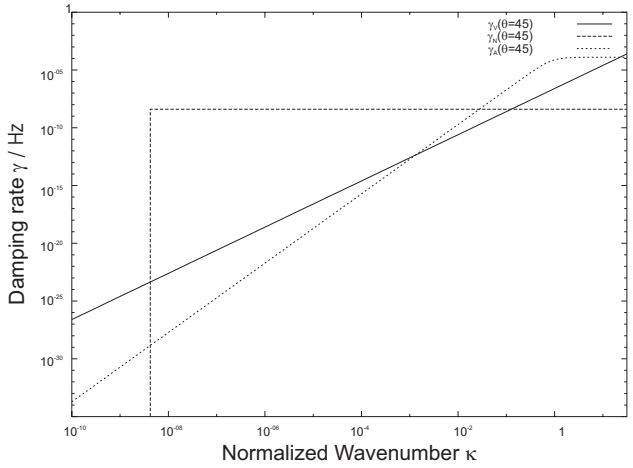

Fig. 5. Comparison of the damping rates at $\theta = 45°$.

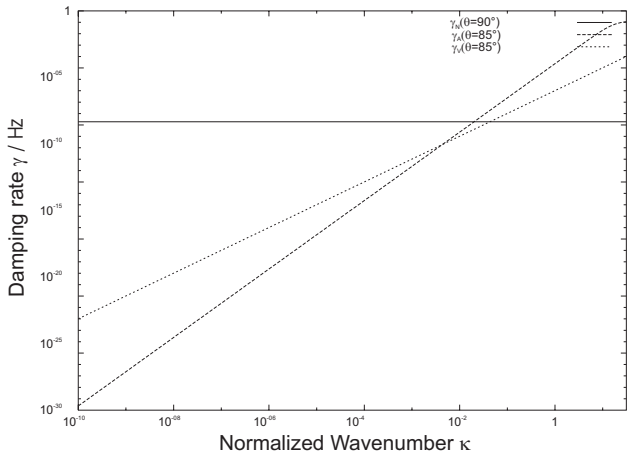

Fig. 6. Comparison of the damping rates at $\theta = 86°$.

3.4. Ion-neutral friction

Kulsrud & Pearce (1969) have derived the damping due to ion-neutral friction for parallel propagating Alfvén waves in a cold interstellar medium. In Appendix C we derive the ion-neutral damping rate for arbitrary propagation angle. We obtain

$$\gamma_N(k) \simeq \nu_N \cos^2\theta \tag{30}$$

for normalised wavenumbers $\kappa \geq \kappa_N \cos\theta$ where $\nu_N = 4 \times 10^{-9} n_H$ Hz and $\kappa_N = 10^{-7} n_H / b_4$. The damping rate (30) holds for nearly all propagation angles $\theta \leq \theta_D$ where

$$\theta_D = \frac{\pi}{2} - \frac{\omega_R}{43\Omega_p} = \frac{\pi}{2} - \frac{\kappa\cos\theta}{43} \geq \frac{\pi}{2} - \frac{\kappa}{43} \tag{31}$$

in terms of the dimensionless wave number (16). In the interesting wave number range of interstellar turbulence $\kappa \leq 1$, the limiting angle (31) is basically equal to 90°, so in the following we adopt the damping rate (30) to hold for all angles.

In Figs. 1–3 we show the individual damping rates $\gamma_A(\kappa)$, $\gamma_{V+J}(\kappa)$ and $\gamma_N(\kappa)$ for the three propagation angles $\theta = 2, 45$ and 85 degrees. Additionally, these three damping rates are compared for any of those angles in Figs. 4–6. It can be seen that at low wavenumbers ion-neutral damping dominates whereas at large wavenumbers Joule and viscous damping dominates at small ($\theta = 2$ degrees) propagation angles, whereas at larger propagation angles Landau damping provides the dominant contribution.

4. Alfvén wave energy loss rates

With the respective damping rates (18), (29) and (30) inserted into Eq. (9) it is straightforward to determine the respective energy loss rates

$$\epsilon_i = C_A^2 k_c^{1-s} \int_{\kappa_{min}}^{\kappa_{max}} d\kappa\, \kappa^{-s-2} \times \int_{-1}^{1} d\mu \frac{1-\mu^2}{\left[\mu^2 + \Lambda(1-\mu^2)\right]^{\frac{2+s}{2}}} \gamma_i(\kappa,\mu) \tag{32}$$

with $\mu = \cos\theta$, $\kappa_{min} = k_{min}/k_c$ and $\kappa_{max} = k_{max}/k_c$. The total energy loss rate is then given by the sum

$$\epsilon_0 = \epsilon_A + \epsilon_{V+J} + \epsilon_N. \tag{33}$$

We discuss each loss rate in turn.

4.1. Landau damping

With the damping rate (17) the Landau damping energy loss rate is

$$\epsilon_{\rm A} = \sqrt{\frac{\pi}{8}}\frac{m_{\rm e}}{m_{\rm p}}v_{\rm e}C_{\rm A}^2k_{\rm c}^{2-s}\int_{\kappa_{\rm min}}^{\kappa_{\rm max}}{\rm d}\kappa\,\kappa^{1-s} \times\int_0^1{\rm d}t\,\frac{(1-t)^2[t+\Lambda(1-t)]^{-\frac{2+s}{2}}}{1-t+3\left(k^2/k_{\rm c}^2\right)t^2}\cdot \quad (34)$$

According to Spangler (1991) the inner and outer scale of the interstellar plasma are $l_{\rm min} = 10^7 l_7$ cm and $l_{\rm max} = 3\times10^{18}L_{\rm pc}$ cm, respectively, so that $\kappa_{\rm max} = 2\pi/l_{\rm min}k_{\rm c} = 31.4l_7^{-1}n_{0.2}^{-1/2}$ and $\kappa_{\rm min} = 2\pi/l_{\rm max}k_{\rm c} = 10^{-10}L_{\rm pc}^{-1}n_{0.2}^{-1/2}$. Obviously, we have a situation with $\kappa_{\rm min} \ll 1 < \kappa_{\rm max}$. We therefore approximate Eq. (34) as

$$\epsilon_{\rm A} \simeq 3.4\times10^{-4}v_{\rm e}C_{\rm A}^2k_{\rm c}^{2-s}\Lambda^{-\frac{2+s}{2}}\left[\int_{\kappa_{\rm min}}^1{\rm d}\kappa\kappa^{1-s}J_1(s,\Lambda) + \frac{k_{\rm c}^2}{3}\int_1^{\kappa_{\rm max}}{\rm d}\kappa\kappa^{-1-s}J_2(s,\Lambda,k,k_{\rm c})\right] \quad (35)$$

where in terms of hypergeometric functions

$$J_1(s,\Lambda) \equiv \int_0^1{\rm d}t\,(1-t)\left[1-\left(1-\Lambda^{-1}\right)t\right]^{-\frac{2+s}{2}} = \frac{1}{2}F\left(1+\frac{s}{2},1;3;1-\Lambda^{-1}\right) \quad (36)$$

and

$$J_2(s,\Lambda,k,k_{\rm c}) \equiv \int_0^1{\rm d}t\,\left[1-\left(1-\Lambda^{-1}\right)t\right]^{-\frac{2+s}{2}}\frac{(1-t)^2}{t^2+\frac{k_{\rm c}^2}{3k^2}(1-t)}\cdot \quad (37)$$

Instead of calculating J_2 exactly, we approximate it from above by noting that $\forall t$

$$\frac{1}{t^2+\frac{k_{\rm c}^2}{3k^2}(1-t)} \le \frac{1}{\frac{k_{\rm c}^2}{3k^2}(1-t)}$$

so that

$$J_2(s,\Lambda,k,k_{\rm c}) \le \frac{3k^2}{k_{\rm c}^2}\int_0^1{\rm d}t(1-t)\left[1-(1-\Lambda^{-1})\right]^{-\frac{2+s}{2}} = \frac{3k^2}{k_{\rm c}^2}J_1(s,\Lambda)\cdot \quad (38)$$

With Eqs. (36) and (38) we obtain an upper limit for the loss rate (35)

$$\epsilon_{\rm A} \le 6.8\times10^{-4}v_{\rm e}C_{\rm A}^2k_{\rm c}^{2-s}\Lambda^{-\frac{2+s}{2}}\frac{\kappa_{\rm max}^{2-s}-\kappa_{\rm min}^{2-s}}{2-s}\cdot \quad (39)$$

With Eq. (6) we derive

$$(\delta B_{\rm A})^2 = \int{\rm d}^3kP_{\rm yy}^{\rm A}(\boldsymbol{k}) = 2\pi C_{\rm A}^2\Lambda^{-(2+s)/2}k_{\rm c}^2\frac{k_{\rm min}^{-(1+s)}-k_{\rm max}^{-(1+s)}}{s+1}J(\Lambda,s) \quad (40)$$

where

$$J(\Lambda,s) \equiv \int_0^1{\rm d}t(1-t)t^{-1/2}\left[1-\left(1-\Lambda^{-1}\right)t\right]^{-(2+s)/2} = \frac{4}{3}F\left(1+\frac{s}{2},\frac{1}{2};\frac{5}{2};1-\Lambda^{-1}\right). \quad (41)$$

Solving Eq. (40) for $C_{\rm A}^2$ yields

$$C_{\rm A}^2 = \frac{s+1}{2\pi}\Lambda^{\frac{s+2}{2}}\frac{(\delta B_{\rm A})^2}{J(\Lambda,s)}k_{\rm c}^{s-1}\frac{\kappa_{\rm min}^{1+s}}{1-\left(\frac{\kappa_{\rm min}}{\kappa_{\rm max}}\right)^{1+s}}\cdot \quad (42)$$

Inserting this result into Eq. (39) we obtain

$$\epsilon_{\rm A} \le 1.1\times10^{-5}\frac{s+1}{2-s}v_{\rm e}k_{\rm c}(\delta B_{\rm A})^2\kappa_{\rm max}^{2-s}\kappa_{\rm min}^{s+1} \times\frac{1-\left(\frac{\kappa_{\rm min}}{\kappa_{\rm max}}\right)^{2-s}}{1-\left(\frac{\kappa_{\rm min}}{\kappa_{\rm max}}\right)^{1+s}}H_{\rm A}(\Lambda,s) \quad (43)$$

with

$$H_{\rm A}(\Lambda,s) = \frac{J_1(\Lambda,s)}{J(\Lambda,s)} = \frac{3}{8}\frac{F\left(1+\frac{s}{2},1;3;1-\Lambda^{-1}\right)}{F\left(1+\frac{s}{2},\frac{1}{2};\frac{5}{2};1-\Lambda^{-1}\right)} = \frac{3}{8}\frac{F\left(1+\frac{s}{2},2;3;1-\Lambda\right)}{F\left(1+\frac{s}{2},2;\frac{5}{2};1-\Lambda\right)} \quad (44)$$

where we used the transformation formula (Abramowitz & Stegun 1972)

$$F(a,b;c;z) = (1-z)^{-a}F\left(a,c-b;c;\frac{z}{z-1}\right)\cdot \quad (45)$$

In Appendix A it is shown that the anisotropy function $H_{\rm A}(\Lambda,s)$ is independent of Λ for large values of $\Lambda \gg 1$ and varies $\propto\Lambda^{1/2}$ for small values of $\Lambda \ll 1$. In the isotropic ($\Lambda = 1$) case we obtain $H_{\rm A}(\Lambda=1,s) = 3/8$ from Eq. (44).

The leading dependence of Eq. (43) for $s < 2$ yields

$$\epsilon_{\rm A}(\Lambda) \simeq 1.1\times10^{-4}\frac{s+1}{2-s}(\delta B_{\rm A})^2v_{\rm e}k_{\rm c}\kappa_{\rm max}^{2-s}\kappa_{\rm min}^{s+1}H(\Lambda,s). \quad (46)$$

4.1.1. Comparison with Landau damping of fast magnetosonic waves

Comparing the Alfvénic Landau damping loss rate (46) for isotropic ($\Lambda = 1$) turbulence with the corresponding loss rate of fast magnetosonic waves from Paper I we derive for the ratio

$$R(\Lambda=1) = \frac{\epsilon_{\rm A}(\Lambda=1)}{\epsilon_{\rm M}(\Lambda=1)} = \frac{(\delta B_{\rm A})^2}{(\delta B_{\rm M})^2}\left(\frac{k_{\rm min}}{k_{\rm c}}\right)^2 = \left(\frac{2\pi}{l_{\rm max}k_{\rm c}}\right)^2\frac{(\delta B_{\rm A})^2}{(\delta B_{\rm M})^2} \simeq 10^{-20}L_{\rm pc}^{-2}\frac{(\delta B_{\rm A})^2}{(\delta B_{\rm M})^2}\cdot \quad (47)$$

For comparable magnetic field energy densities the Alfvénic Landau energy loss rate in the isotropic turbulence case is twenty orders of magnitude smaller than the corresponding magnetosonic energy loss rate, and thus negligibly small.

The Alfvénic Landau damping energy loss rate is also negligibly small compared to the magnetosonic Landau damping energy loss rate for anisotropic turbulence as long as

$$\left[10^{-20}L_{\rm pc}^{-2}\frac{(\delta B_{\rm A})^2}{(\delta B_{\rm M})^2}\right]^{2/s} \ll \Lambda \ll \left[10^{20}L_{\rm pc}^{2}\frac{(\delta B_{\rm M})^2}{(\delta B_{\rm A})^2}\right]^{2/s}. \quad (48)$$

For $\Lambda \gg 1$, $\epsilon_{\rm M} \propto \Lambda^{-s/2}$ (see Paper I) so that

$$R(\Lambda \gg 1) \simeq R(\Lambda = 1)\Lambda^{s/2} = 10^{-20}L_{\rm pc}^{-2}\Lambda^{s/2}\frac{(\delta B_{\rm A})^2}{(\delta B_{\rm M})^2}. \quad (49)$$

For small values $\Lambda \ll 1$ we obtain with $\epsilon_{\rm M} \propto \Lambda^{(1+s)/2}$ (correcting an error in Eq. (30) of Paper I)

$$R(\Lambda \ll 1) \simeq R(\Lambda = 1)\Lambda^{-s/2} = 10^{-20}L_{\rm pc}^{-2}\Lambda^{-s/2}\frac{(\delta B_{\rm A})^2}{(\delta B_{\rm M})^2}. \quad (50)$$

The requirements $R(\Lambda) \leq 1$ in Eqs. (49) and (50) immediately yield the constraints (48).

4.1.2. Numerical value for intercloud plasma parameters

For typical intercloud plasma and turbulence parameters, $s = 5/3$, $(\delta B_{\rm A}) = 0.9\,\mu$G and values given above, the Alfvénic Landau energy loss rate (46) becomes

$$\epsilon_{\rm A}(\Lambda) \simeq 3.8\times 10^{-42}\, T_4^{1/2}\, n_{0.2}^{-1}\, l_7^{-1/2}\, L_{\rm pc}^{-8/3}$$

$$(\delta B_{\rm A}/0.9\,\mu{\rm G})^2 H_{\rm A}(\Lambda, 5/3)\ {\rm erg\ cm^{-3}\ s^{-1}}. \quad (51)$$

4.2. Joule and viscous damping

With the Joule and viscous damping rate (29) we obtain from Eq. (32) for the corresponding energy loss rate

$$\epsilon_{\rm V+J} = 2.5\times 10^{8} C_{\rm A}^2 n_{0.2} T_4^{-3/2} b_4^{-4} k_{\rm c}^{3-s}\int_{\kappa_{\rm min}}^{\kappa_{\rm max}} {\rm d}\kappa\kappa^{-s} \times \int_0^1 {\rm d}t\,\frac{(1-t)(1+3t)}{[t+\Lambda(1-t)]^{\frac{2+s}{2}}} = \frac{2.5\times 10^8}{s-1} C_{\rm A}^2 n_{0.2} T_4^{-3/2} \times b_4^{-4} k_{\rm c}^{3-s}\Lambda^{-\frac{2+s}{2}}\kappa_{\rm min}^{1-s}\left[1-\left(\frac{\kappa_{\rm min}}{\kappa_{\rm max}}\right)^{s-1}\right] J_3(\Lambda, s) \quad (52)$$

where in terms of hypergeometric functions and Eq. (36)

$$J_3(\Lambda, s) = J_1(\Lambda, s) + \frac{1}{2}F\left(1+\frac{s}{2}, 2; 4; 1-\Lambda^{-1}\right) = \frac{1}{2}\left[F\left(1+\frac{s}{2}, 1; 3; 1-\Lambda^{-1}\right) + F\left(1+\frac{s}{2}, 2; 4; 1-\Lambda^{-1}\right)\right]. \quad (53)$$

Using again (42) we derive

$$\epsilon_{\rm V+J} = 4\times 10^7 \frac{s+1}{s-1} n_{0.2} T_4^{-3/2} b_4^{-4} (\delta B_{\rm A})^2 k_{\rm c}^2 \kappa_{\rm min}^2 \times \frac{1-\left(\frac{\kappa_{\rm min}}{\kappa_{\rm max}}\right)^{s-1}}{1-\left(\frac{\kappa_{\rm min}}{\kappa_{\rm max}}\right)^{s+1}} H_{\rm V+J}(\Lambda, 5/3) \quad (54)$$

with

$$H_{\rm V+J}(\Lambda, s) = H_{\rm A}(\Lambda, s) + h_{\rm V+J}(\Lambda, s) \quad (55)$$

and

$$h_{\rm V+J}(\Lambda, s) = \frac{3}{8}\frac{F\left(1+\frac{s}{2}, 2; 4; 1-\Lambda^{-1}\right)}{F\left(1+\frac{s}{2}, \frac{1}{2}; \frac{5}{2}; 1-\Lambda^{-1}\right)} = \frac{3}{8}\frac{F\left(1+\frac{s}{2}, 2; 4; 1-\Lambda\right)}{F\left(1+\frac{s}{2}, 2; \frac{5}{2}; 1-\Lambda\right)}. \quad (56)$$

In Appendix B it is shown that the anisotropy function $H_{\rm V+J}(\Lambda, s)$ is independent of Λ for large values of $\Lambda \gg 1$ and varies $\propto\Lambda^{1/2}$ for small values of $\Lambda \ll 1$. In the isotropic ($\Lambda = 1$) case we obtain $H_{\rm J+V}(\Lambda = 1, s) = 3/8$ from Eq. (55). The leading dependence of Eq. (54) for $s > 1$ yields

$$\epsilon_{\rm V+J} = 4\times 10^7 \frac{s+1}{s-1} n_{0.2} T_4^{-3/2} b_4^{-4} (\delta B_{\rm A})^2 k_{\rm c}^2 \kappa_{\rm min}^2 H_{\rm V+J}(\Lambda, s). \quad (57)$$

For typical intercloud plasma and turbulence parameters we obtain

$$\epsilon_{\rm V+J} = 1\times 10^{-39} n_{0.2} T_4^{-3/2} b_4^{-4} L_{\rm pc}^{-2} \times (\delta B_{\rm A}/0.9\,\mu{\rm G})^2\, H_{\rm V+J}(\Lambda, s)\ {\rm erg\ cm^{-3}\ s^{-1}} \quad (58)$$

which is a factor 500 larger than the Landau damping rate (51) of Alfvén waves.

4.3. Ion-neutral damping

With the ion-neutral damping rate (30) we obtain from Eq. (32) for the corresponding energy loss rate

$$\epsilon_{\rm N} = C_{\rm A}^2 k_{\rm c}^{1-s}\nu_{\rm N}\int_0^1 {\rm d}t\,\frac{(1-t)t^{1/2}}{[t+\Lambda(1-t)]^{\frac{2+s}{2}}} \times \int_{\max[\kappa_{\rm N}t^{1/2}, \kappa_{\rm min}]}^{\kappa_{\rm max}} {\rm d}\kappa\kappa^{-s-2}. \quad (59)$$

If we introduce

$$t_{\rm E} = \left(\frac{\kappa_{\rm min}}{\kappa_{\rm N}}\right)^2 = 10^{-6}\frac{b_4^2}{n_{\rm H}^2 L_{\rm pc}^2 n_{0.2}} \quad (60)$$

the loss rate (59) in the limit $\kappa_{\rm max} \gg \kappa_{\rm min}$ and $\kappa_{\rm max} \gg \kappa_{\rm N}$ becomes

$$\epsilon_{\rm N} \simeq \frac{C_{\rm A}^2 k_{\rm c}^{1-s}\nu_{\rm N} x_{\rm min}^{-s-1}}{s+1}\left[\int_0^{t_{\rm E}} {\rm d}t\,\frac{(1-t)t^{1/2}}{[t+\Lambda(1-t)]^{\frac{2+s}{2}}} + t_{\rm E}^{(s+1)/2}\int_{t_{\rm E}}^1 {\rm d}t\,\frac{(1-t)t^{-s/2}}{[t+\Lambda(1-t)]^{\frac{2+s}{2}}}\right] = \frac{\nu_{\rm N}\Lambda^{\frac{2+s}{2}}}{2\pi J(\Lambda, s)}(\delta B_{\rm A})^2\left[\int_0^{t_{\rm E}} {\rm d}t\,\frac{(1-t)t^{1/2}}{[t+\Lambda(1-t)]^{\frac{2+s}{2}}} + t_{\rm E}^{(s+1)/2}\int_{t_{\rm E}}^1 {\rm d}t\,\frac{(1-t)t^{-s/2}}{[t+\Lambda(1-t)]^{\frac{2+s}{2}}}\right] = \frac{\nu_{\rm N}\Lambda^{\frac{2+s}{2}}}{2\pi J(\Lambda, s)}(\delta B_{\rm A})^2\left[\frac{4t_{\rm E}^{(s+1)/2}}{(4-s)(2-s)\Lambda^{(2+s)/2}} \times F\left(1+\frac{s}{2}, 1-\frac{s}{2}; 3-\frac{s}{2}; 1-\Lambda^{-1}\right) + \int_0^{t_{\rm E}} {\rm d}t\,\frac{(1-t)\left(t^{1/2}-t_{\rm E}^{(s+1)/2}t^{-s/2}\right)}{[t+\Lambda(1-t)]^{\frac{2+s}{2}}}\right]. \quad (61)$$

For values of $s < 2$ the remaining integral in Eq. (61) in the limit $t_E < \Lambda$ and $t_E \ll 1$ can be well approximated as

$$\int_0^{t_E} \mathrm{d}t \frac{(1-t)\left(t^{1/2} - t_E^{(s+1)/2} t^{-s/2}\right)}{[t+\Lambda(1-t)]^{\frac{2+s}{2}}} \simeq \int_0^{t_E} \mathrm{d}t \left(t^{1/2} - t_E^{(s+1)/2} t^{-s/2}\right) = -\frac{2(s+1)}{3(2-s)} t_E^{3/2}$$

so that Eq. (61) reduces to

$$\epsilon_N \simeq \frac{\nu_N (\delta B_A)^2 t_E^{(s+1)/2}}{2\pi(2-s)\Lambda^{\frac{2+s}{2}} J(\Lambda, s)} \times \left[\frac{4}{4-s} F\left(1+\frac{s}{2}, 1-\frac{s}{2}; 3-\frac{s}{2}; 1-\Lambda^{-1}\right) - \frac{2(s+1)}{3} t_E^{2-s/2}\right] \simeq \frac{2\nu_N (\delta B_A)^2 t_E^{(s+1)/2}}{\pi(2-s)(4-s)\Lambda^{\frac{2+s}{2}} J(\Lambda, s)} \times F\left(1+\frac{s}{2}, 1-\frac{s}{2}; 3-\frac{s}{2}; 1-\Lambda^{-1}\right) \quad (62)$$

because for $t_E \ll 1$ and $s < 2$ the second term can be neglected compared to the first term. Introducing the anisotropy function

$$H_N(\Lambda, s) = \frac{F\left(1+\frac{s}{2}, 1-\frac{s}{2}; 3-\frac{s}{2}; 1-\Lambda^{-1}\right)}{J(\Lambda, s)} = \frac{3F\left(1+\frac{s}{2}, 2; 3-\frac{s}{2}; 1-\Lambda\right)}{4F\left(1+\frac{s}{2}, 2; \frac{5}{2}; 1-\Lambda\right)} \quad (63)$$

we arrive at

$$\epsilon_N \simeq \frac{2}{\pi(2-s)(4-s)} \nu_N t_E^{(s+1)/2} (\delta B_A)^2 H_N(\Lambda, s). \quad (64)$$

By the same methods as before we obtain in the isotropic ($\Lambda = 1$) case $H_N(\Lambda = 1, s) = 3/4$ from Eq. (63). For large values of $\Lambda \gg 1$ the anisotropy function approaches the constant $H_N(\Lambda \gg 1) \simeq \frac{2^{s-3}(4-s)(2-s)\sqrt{\pi}}{\Gamma(1+\frac{s}{2})}$, whereas for small values of $\Lambda \ll 1$ the anisotropy function

$$H_N(t_E < \Lambda \ll 1) \simeq \frac{(s+1)}{(4-s)(2-s)^2} \Lambda^{-s/2} \quad (65)$$

increases $\propto \Lambda^{-s/2}$.

Numerically we obtain for isotropic turbulence and $s = 5/3$

$$\epsilon_N \simeq 1.74 \times 10^{-29} n_H^{-5/3} b_4^{8/3} L_{pc}^{-8/3} n_{0.2}^{-4/3} \text{ erg cm}^{-3} \text{ s}^{-1} \quad (66)$$

which is 13 orders of magnitude larger than the Landau damping rate (51) of Alfvén waves, and 10 orders of magnitude larger than the viscous and Joule damping rate (58) of Alfvén waves.

5. Summary and conclusions

We have calculated the heating rate of the diffuse intercloud medium from the dissipation of interstellar shear Alfvén waves. Relating the Alfvénic magnetic field fluctuation power spectrum to the observed interstellar electron density fluctuation power spectrum we derive the heating rate allowing for a scale independent anisotropy of the power spectrum. Because the diffuse intercloud medium is a partially ionised medium, the shear Alfvén waves undergo different types of dissipation. Besides collisionless Landau damping we considered various damping mechanisms from collision-effects such as Joule dissipation, electron and ion viscosity and ion-neutral friction.

For all individual damping processes we derive the respective damping rates as a function of wavenumber and propagation angles of the Alfvén waves. These damping rates then serve as input in the calculation of the associated heating rates of the intertellar medium which results from the integral over the product of the damping rate times the magnetic field fluctuation power spectrum allowing for a scale independent anisotropy of the power spectrum.

We demonstrate that for isotropic turbulence and typical diffuse intercloud medium parameters ion-neutral friction provides the dominant contribution to the heating rate of about 10^{-29} erg cm^{-3} s^{-1}, which is about four orders of magnitude smaller than the cooling rate of the diffuse intercloud medium. Heating by collisionless Landau damping is 13 orders of magnitude smaller than dissipation by ion-neutral friction, heating by Joule and viscosity dissipation is 10 orders of magnitude smaller. Apart from factors of order unity these heating rates also hold for predominantly parallel turbulence ($\Lambda \gg 1$). In case of predominantly perpendicular turbulence ($\Lambda \ll 1$) the heating rates from collisionless Landau damping and Joule and viscosity dissipation decrease $\propto \Lambda^{1/2}$, whereas the heating rate from ion-neutral friction increases $\propto \Lambda^{-s/2}$ as long as $\Lambda \geq 10^{-6}$.

We also have compared the Alfvén wave heating rate with the previously calculated collisionless Landau damping rate of fast magnetosonic waves:

(1) in the isotropic case for standard turbulence parameters of the diffuse interstellar medium the collisionless Alfvén heating rate is seventeen orders of magnitude smaller than the collisionless magnetosonic heating rate;

(2) in the isotropic case the total Alfvén wave heating rate is four orders of magnitude smaller than the collisionless magnetosonic heating rate.

Hence, for the temperature balance of the warm intercloud medium heating from shear Alfvén waves is negligible compared to the heating by collisionless damping of fast magnetosonic waves.

In future work we will also determine the contributions from Joule dissipation, electron and ion viscosity dissipation and ion-neutral friction dissipation of fast magnetosonic waves to arrive at a complete description of interstellar medium heating by wave dissipation processes.

Acknowledgements. We thank the anonymous referee for his very constructive and helpful report. M.L. gratefully acknowledges support as young researcher of the PLATON network (EC contract HPRN-CT-2000-00153). F.S. and R.S. acknowledge partial support by the Deutsche Forschungsgemeinschaft through Sonderforschungsbereich 591.

Appendix A: Approximations of the anisotropy function $H_A(\Lambda, s)$

In the isotropic case ($\Lambda = 1$) we obtain from Eq. (44) $H_A(\Lambda = 1, s) = 3/8$.

Moreover, using

$$F(a, b; c; 1) = \frac{\Gamma(c)\Gamma(c-a-b)}{\Gamma(c-a)\Gamma(c-b)} \tag{67}$$

for $c \neq 0, -1. - 2, ...$, $\Re(c-a-b) > 0$, we find that the Alfvénic Landau damping heating rate does not vary significantly for large ($\Lambda \gg 1$) values of the anisotropy parameter, resembling parallel turbulence:

$$H_A(\Lambda \gg 1, s) \simeq \frac{3}{8}\frac{F\left(1+\frac{s}{2}, 1; 3; 1\right)}{F\left(1+\frac{s}{2}, \frac{1}{2}; \frac{5}{2}; 1\right)} = \frac{2}{(2-s)\pi^{1/2}}\frac{\Gamma\left(\frac{3-s}{2}\right)}{\Gamma\left(\frac{2-s}{2}\right)}. \tag{68}$$

In case of small ($\Lambda \ll 1$) values of the anisotropy parameter, resembling perpendicular turbulence, we approximate the integrals $J_1(\Lambda, s)$ and $J(\Lambda, s)$ as

$$\begin{aligned} J_1(s, \Lambda \ll 1) &= \int_0^1 \mathrm{d}t\,(1-t)\left[1-\left(1-\Lambda^{-1}\right)t\right]^{-\frac{2+s}{2}} \\ &\simeq \int_0^1 \mathrm{d}t\,(1-t)[1+(t/\Lambda)]^{-\frac{2+s}{2}} \\ &\simeq \int_0^\Lambda \mathrm{d}t(1-t) + \Lambda^{(2+s)/2}\int_\Lambda^1 \mathrm{d}t(1-t)t^{-(2+s)/2} \\ &\simeq \frac{2+s}{2}\Lambda \end{aligned} \tag{69}$$

and

$$\begin{aligned} J(s, \Lambda \ll 1) &= \int_0^1 \mathrm{d}t\,(1-t)t^{-1/2}\left[1-\left(1-\Lambda^{-1}\right)t\right]^{-\frac{2+s}{2}} \\ &\simeq \int_0^1 \mathrm{d}t\,t^{-1/2}(1-t)[1+(t/\Lambda)]^{-\frac{2+s}{2}} \\ &\quad + \int_0^\Lambda \mathrm{d}t(1-t)t^{-1/2} \\ &\quad + \Lambda^{(2+s)/2}\int_\Lambda^1 \mathrm{d}t(1-t)t^{-(3+s)/2} \\ &\simeq \frac{2(2+s)}{1+s}\Lambda^{1/2}, \end{aligned} \tag{70}$$

respectively. For the ratio we then find

$$H_A(\Lambda \ll 1, s) = \frac{J_1(\Lambda \ll 1, s)}{J(\Lambda \ll 1, s)} = \frac{1+s}{4}\Lambda^{1/2}. \tag{71}$$

Appendix B: Approximations of the anisotropy function $H_{V+J}(\Lambda, s)$

Using again Eq. (67) for large values of $\Lambda \gg 1$ we approximate

$$F\left(1+\frac{s}{2}, 2; 4; 1-\Lambda^{-1}\right) \simeq F\left(1+\frac{s}{2}, 2; 4; 1\right) = \frac{48}{(4-s)(2-s)^2\Gamma\left[\frac{2-s}{2}\right]} \tag{72}$$

and

$$F\left(1+\frac{s}{2}, \frac{1}{2}; \frac{5}{2}; 1-\Lambda^{-1}\right) \simeq F\left(1+\frac{s}{2}, \frac{1}{2}; \frac{5}{2}; 1\right) = \frac{3\pi^{1/2}\Gamma\left[\frac{2-s}{2}\right]}{4\Gamma\left[\frac{3-s}{2}\right]} \tag{73}$$

so that

$$h_{V+J}(\Lambda \gg 1, s) \simeq \frac{64\Gamma\left[\frac{3-s}{2}\right]}{(4-s)(2-s)^2\Gamma^2\left[\frac{2-s}{2}\right]}. \tag{74}$$

According to Eqs. (55) and (68) we then derive

$$H_{V+J}(\Lambda \gg 1, s) \simeq \frac{2}{(2-s)\pi^{1/2}}\frac{\Gamma\left(\frac{3-s}{2}\right)}{\Gamma\left(\frac{2-s}{2}\right)} \times\left[1+\frac{32}{(4-s)(2-s)\Gamma\left[\frac{2-s}{2}\right]}\right]. \tag{75}$$

For small values of $\Lambda \ll 1$ we approximate from Eq. (53) with Eqs. (45) and (72)

$$\begin{aligned} F\left(1+\frac{s}{2}, 2; 4; 1-\Lambda^{-1}\right)] &= \Lambda^{\frac{2+s}{2}}F\left(1+\frac{s}{2}, 2; 4; 1-\Lambda\right] \\ &\simeq \Lambda^{\frac{2+s}{2}}F\left(1+\frac{s}{2}, 2; 4; 1\right) \\ &= \frac{48}{(4-s)(2-s)^2\Gamma\left[\frac{2-s}{2}\right]}\Lambda^{\frac{2+s}{2}}. \end{aligned} \tag{76}$$

Together with approximations (69) and (70) we then obtain according to Eq. (55)

$$\begin{aligned} H_{V+J}(\Lambda \ll 1, s) &\simeq \frac{\frac{2+s}{2}\Lambda}{\frac{2(2+s)\Lambda^{1/2}}{1+s}} \times\left[1+\frac{48}{(4-s)(2+s)(2-s)^2\Gamma\left[\frac{2-s}{2}\right]}\Lambda^{\frac{s}{2}}\right] \\ &\simeq \frac{1+s}{4}\Lambda^{1/2} = H_A(\Lambda \ll 1, s) \end{aligned} \tag{77}$$

the same asymptotic behaviour at small Λ as for $H_A(\Lambda \ll 1, s)$.

Appendix C: Derivation of the angular dependence of ion-neutral damping

The dispersion relation of low-frequency transverse waves in a cold interstellar medium has been derived in Ch. 9.2.7 of Schlickeiser (2002). According to Eqs. (9.2.96)–(9.2.28) of Schlickeiser (2002) we obtain for Alfvén waves

$$N^2 = \frac{S\left(1+\cos^2\theta\right) - |S|\sqrt{\sin^4\theta + \frac{4}{v}\cos^2\theta}}{2\cos^2\theta\left(1+\frac{\xi}{v-1}\tan^2\theta\right)} \tag{78}$$

where $v = \Omega_p^2/\omega^2$ and $\xi = m_e/m_p = 1/1836$. The behaviour of the dispersion relation (78) is controlled by the two characteristic angles θ_c and θ_D, where

$$\sin^4\theta_c = \frac{4}{v}\cos^2\theta_c \tag{79}$$

yielding

$$\theta_{\rm c} = \arccos\left[\sqrt{1+v^{-1}} - v^{-1/2}\right], \tag{80}$$

and

$$\tan^2\theta_{\rm D} = \frac{|v-1|}{\xi} \tag{81}$$

yielding

$$\theta_{\rm D} = \arctan\left[43\sqrt{|v-1|}\right]. \tag{82}$$

At frequencies much below the ion cyclotron frequency $v \gg 1$, implying

$$\begin{aligned}\theta_{\rm c} &\simeq \arccos\left[1-v^{-1/2}\right] \simeq \arcsin\left(2^{1/2}v^{-1/4}\right)\\ &\simeq 2^{1/2}v^{-1/4} = \sqrt{\frac{2\omega}{\Omega_{\rm p}}}\end{aligned} \tag{83}$$

and

$$\theta_{\rm D} \simeq \arctan\left(43v^{1/2}\right) \simeq \frac{\pi}{2} - \frac{1}{43v^{1/2}} = \frac{\pi}{2} - \frac{\omega}{43\Omega_{\rm p}}. \tag{84}$$

At low-frequencies we therefore can consider two ranges of propagation angles:
(1) small propagation angles $\theta \ll \theta_{\rm c} \ll \theta_{\rm D}$ corresponding to

$$\theta \ll \sqrt{\frac{2\omega}{\Omega_{\rm p}}} \ll \frac{\pi}{2} - \frac{\omega}{43\Omega_{\rm p}}. \tag{85}$$

Here the dispersion relation (78) simplifies to

$$N^2 \simeq \frac{S\left(1+\cos^2\theta\right) - |S|\frac{2}{v^{1/2}}\cos\theta}{2\cos^2\theta} \simeq S \tag{86}$$

(2) large propagation angles $\theta_{\rm c} \ll \theta \ll \theta_{\rm D}$ corresponding to

$$\sqrt{\frac{2\omega}{\Omega_{\rm p}}} \ll \theta \ll \frac{\pi}{2} - \frac{\omega}{43\Omega_{\rm p}}. \tag{87}$$

Here the dispersion relation (78) simplifies to

$$N^2 \simeq \frac{S\left(1+\cos^2\theta\right) - |S|\sin^2\theta}{2\cos^2\theta} = S, \tag{88}$$

which equals approximation (86).

At low plasma frequencies $\omega \ll \Omega_{\rm p}$ we therefore use the dispersion relation

$$N_\pm^2 = \frac{S}{\cos^2\theta} \tag{89}$$

for all propagation angles $\theta \le \theta_{\rm D} = \frac{\pi}{2} - \frac{\omega}{43\Omega_{\rm p}}$ which is very close to 90°.

The Stix parameter S is given by

$$S = 1 - \sum_{\rm a}\frac{\omega_{\rm pa}^2}{\omega}\left(\frac{1}{\omega-\Omega_{\rm a}} + \frac{1}{\omega+\Omega_{\rm a}}\right). \tag{90}$$

Now we introduce collisions with neutrals by substituting

$$\frac{1}{\omega \pm \Omega_{\rm a}} \to \frac{1}{\omega + \imath\nu_{\rm a} \pm \Omega_{\rm a}} \tag{91}$$

where $\nu_{\rm a}$ is the collision frequency of species a with the neutrals.

To derive the damping rate (Γ) in the weak damping limit ($\Gamma \ll \omega_{\rm R}$) we substitute $\omega = \omega_{\rm R} + \imath\Gamma$. The standard Taylor expansion around $\Gamma = 0$ yields for the real part of the index of refraction

$$N_{\rm R}^2 = \frac{c^2k^2}{\omega_{\rm R}^2} = \frac{S(\omega_{\rm R})}{\cos^2\theta} \tag{92}$$

and for the damping rate

$$\Gamma = -\frac{\omega_{\rm R}^2\left(\nu_{\rm e}\Omega_{\rm e}^2\Omega_{\rm i}^2 + \nu_{\rm i}\Omega_{\rm e}^2\Omega_{\rm i}^2 + \nu_{\rm e}\Omega_{\rm i}^2\omega_{\rm R}^2 + \nu_{\rm i}\Omega_{\rm e}^2\omega_{\rm R}^2\right)}{k_\parallel^2 v_{\rm A}^2\Omega_{\rm e}^2\Omega_{\rm i}^2 + 2\omega_{\rm R}^4\left(\Omega_{\rm e}^2+\Omega_{\rm i}^2\right)}, \tag{93}$$

where we neglected terms of order $\frac{\omega_{\rm R}}{\Omega_{\rm a}} \ll 1$ and $\frac{\nu_{\rm a}}{\Omega_{\rm a}} \ll 1$. Equation (92) immediately leads to

$$\omega_{\rm R}^2 = k_\parallel^2 V_{\rm A}^2 = k^2 V_{\rm A}^2\cos^2\theta. \tag{94}$$

Inserting this into Eq. (93) gives

$$\Gamma_{\rm N} = -\nu_{\rm N}\cos^2\theta \tag{95}$$

as the dominant term for the ion-neutral damping. According to Kulsrud & Pearce (1969) $\nu_{\rm N} = 4\times10^{-9}n_{\rm H}$ Hz.

For interstellar medium parameters Eq. (94) in terms of the dimensionless wavenumber (16) corresponds to

$$|\omega_{\rm R}| = \Omega_{\rm p}\kappa\cos\theta = 0.04b_4\cos\theta\kappa. \tag{96}$$

The weak-damping approximation $|\Gamma_{\rm N}| \le |\omega_{\rm R}|$ then holds at normalised wavenumber greater than

$$\kappa \ge \kappa_{\rm N}\cos\theta \tag{97}$$

where $\kappa_{\rm N} = 10^{-7}n_{\rm H}/b_4$ which is about three orders of magnitude larger than $\kappa_{\rm min}$.

References

Abramowitz, M., & Stegun, I. A. 1972, Handbook of Mathematical Functions (Washington: National Bureau of Standards)
Braginskii, S. I. 1965, Rev. Plasma Phys., 1, 205
Cheng, K.-P., & Bruhweiler, F. C. 1990, ApJ, 364, 573
Cho, J., Lazarian, A., & Vishniac, E. T. 2002, ApJ, 564, 291
Gary, S. P. 1986, J. Plasma Phys., 35, 431
Ginzburg, V. I. 1961, Propagation of Electromagnetic Waves in Plasma (New York: Pergamon Press)
Goldreich, P., & Sridhar, S. 1995, ApJ, 438, 763
Hollweg, J. V. 1985, J. Geophys. Res., 90, 7620
Kulsrud, R. M., & Pearce, W. P. 1969, ApJ, 156, 445
Lerche, I., & Schlickeiser, R. 1982, MNRAS, 201, 1041
Lerche, I., & Schlickeiser, R. 2001, A&A, 366, 1008 (Paper I)
Lerche, I., & Schlickeiser, R. 2002, A&A, 383, 319
Minter, A. H., & Spangler, S. R. 1997, ApJ, 485, 182
Schlickeiser, R., & Lerche, I. 2002, J. Plasma Phys., 68, 191
Schlickeiser, R. 2002, Cosmic Ray Astrophysics (Springer Verlag)
Spangler, S. R. 1991, ApJ, 376, 540
Sturrock, P. A. 1994, Plasma Physics (Cambridge University Press)